

Parameterization of the sea spray generation function with whitecap coverage

Jian Shi^{1*}, Wenjing Zhang¹, Xueyan Zhang¹, Jingdong Liu^{1,2}, Zhenyu Liu¹

¹ College of Meteorology and Oceanography, National University of Defense Technology, Nanjing 211101, China

² Unit 91604 of the Chinese People's Liberation Army, Longkou 265700, China

Received 21 March 2020; accepted 20 May 2020

© Chinese Society for Oceanography and Springer-Verlag GmbH Germany, part of Springer Nature 2020

Abstract

Sea spray droplets are produced by waves breaking on the sea surface, and they vary the transfer of energy between the atmosphere and ocean. The sea spray generation function (SSGF) is generally considered as a function of the initial radius of the spray droplets and the wind speed. However, ocean waves always exist at the air-sea interface, so it is not reasonable to consider only the effect of sea surface winds while ignoring the effects of ocean waves. Whitecap coverage is an important characteristic parameter of breaking waves, and researchers believe that this parameter is related to both wave state and wind speed. In this paper, the SSGF is parameterized by the whitecap coverage, and a new SSGF describing different droplet radii is organically integrated based on the whitecap coverage parameter. Then, with the relationship between the whitecap coverage and wave state, the influence of ocean waves on the SSGF for different wave states was analyzed by using observational data in the laboratory. The results show that the new SSGF that considers wave effects can reasonably describe the droplet generation process under different wave state conditions.

Key words: sea spray generation function, whitecap coverage, wave state

Citation: Shi Jian, Zhang Wenjing, Zhang Xueyan, Liu Jingdong, Liu Zhenyu. 2020. Parameterization of the sea spray generation function with whitecap coverage. *Acta Oceanologica Sinica*, 39(8): 24–33, doi: 10.1007/s13131-020-1618-9

1 Introduction

Ocean waves are produced by the ocean winds. As the wind speed increases, the waves break, and tiny spray droplets leave the waves. The existence of sea spray droplets changes and influences the energy transfer between atmosphere and ocean. Furthermore, it affects the prediction of typhoon intensity and climate change which are closely related to the ocean (Liu et al., 2011; Wu et al., 2015; Rizza et al., 2018; Barthel et al., 2019). Sea spray droplets can be divided into two types: one is produced by the collapse of the bubble, and the other is mainly produced by the wind blowing against the wave crest (Veron, 2015). Breaking waves produce many bubbles in the sea, and when a bubble rises to the sea surface, it bursts and produces hundreds of film droplets. After the bubbles burst, a collapsing cavity is filled with surrounding water, then, the water rebounds rapidly as a column, and jet droplets are formed. The radius of bubble-induced film droplets and jet droplets ranges from 3–20 μm . Wind tears the wave crest and carries the droplets away, or the crest of a breaking wave curls over and causes the droplets to leave the main body, this type of droplets is called spume droplets, with a minimum radius generally of approximately 20 μm (Andreas et al., 1995; Veron, 2015).

Andreas (1992) and Fairall et al. (1994, 2009) pointed out that the formulas for calculating the momentum and heat of sea spray droplets used to quantitatively calculate the influence of droplets are mainly based on a SSGF, and the SSGF has a substantial influence on the momentum and heat flux of droplets. Several researchers have proposed that different SSGFs are mainly related

to wind speed (Ling et al., 1980; Smith et al., 1993; Andreas, 1998). The research shows that there are various functions related to wind speed in different SSGFs, and these different functions also have considerable differences in magnitude (Veron, 2015). Zhao et al. (2006) proposed an SSGF that takes into account the influence of wave state, and gave the parameter of wave state for parameterized SSGF. Many researchers found that the influence of waves on SSGF could not be ignored (Mueller and Veron, 2009; Veron et al., 2012; Troitskaya et al., 2018; Lausac et al., 2018). Several different wave state parameters have been used to parameterize the SSGF, and choosing the appropriate wave-state parameters is a problem that has been discussed (Zhao and Toba, 2001; Shi et al., 2011). Zhao et al. (Zhao et al., 2006; Zhao and Toba, 2001) suggested that windsea Reynolds numbers R_B , as wave state parameters, can be effectively used for the parameterization of whitecap coverage and SSGF.

The SSGF is also related to the size spectrum of the droplets (Norris et al., 2013b; Zhao et al., 2006; Andreas, 2004; Veron, 2015; Wan et al., 2017). The investigation of bubble induced droplets is required for modeling cloud microphysical properties and aerosol radiative influences (Callaghan, 2013; Norris et al., 2013a), and the bubble induced droplets have little influence on the air-sea momentum and heat fluxes. However, when it comes to the study of air-sea momentum and heat fluxes, the researchers are more concerned with spume droplets, and the spume droplets influence on the air-sea momentum and heat fluxes are significantly stronger than the bubbles induced droplets (Zhao et al., 2006; Veron, 2015). Thus, due to different research objectives,

Foundation item: The National Natural Science Foundation of China under contract No. 41676014.

*Corresponding author, E-mail: shijian.mil@163.com

SSGF produced by bubble induced droplets and spume droplets are often studied separately, and the corresponding size spectrum of the droplets is discontinuous (Shi et al., 2009, 2016; Liu et al., 2011). However, in the process of droplet generation, the size spectrum of the droplets should be continuous.

Wave breaking is the main way of wave energy dissipation, and the parameterization of wave breaking is also very important in wave simulation (Shao et al., 2018; Sheng et al., 2019). The most direct apparent phenomenon of breaking waves is the appearance of whitecaps on the sea surface. The whitecaps are closely related to the amount of droplets generated by the breaking waves. Whitecap coverage is a characteristic parameter that describes the degree of wave breakage, and is often used to parameterize the SSGF (Monahan and Muircheartaigh 1980; Monahan et al., 1986; Fairall et al., 1994; Norris et al., 2013a). Various investigators have attempted to describe whitecap coverage in terms of wind speed (Monahan et al., 1986; Lafon et al., 2007; Ren et al., 2016). Zhao and Toba (2001), Lafon et al. (2007) analyzed the relationship between whitecap coverage and wind waves, and gave detailed parameterized expressions, pointing out that whitecap coverage had a strong correlation with wind waves. It can be seen that the whitecap coverage parameter is a type of parameter that can represent the effect of wind and waves on the sea surface. In this paper, based on the whitecap coverage, a new SSGF is parameterized, and the influence of ocean waves on the SSGF under different wave conditions is analyzed by combining the relationship between the whitecap coverage and the wave state parameters.

2 Model description

2.1 Parameterization of the sea spray generation function

The amount of sea spray droplets generation is often expressed by the sea spray droplet production rate F , which defined as the number of droplets generated per unit time and area. The F is different for different droplet sizes. Therefore, a function which represents units of number of spray droplets produced per square meter of surface per second per micrometer increment in droplet radius is produced, and it is called SSGF. SSGF is generally regarded as a function of the initial radius, r_0 , and the 10 m wind speed, U_{10} (Ling et al., 1980; Smith et al., 1993; Andreas, 1998). If the sea droplets scale spectrum is not related to the wind speed, it can be considered that SSGF is divided into two independent parts: $f_1(U_{10})$ is the function related only to the wind speed, and $f_2(r_0)$ is the size spectrum of the droplets:

$$\frac{dF}{dr_0} = f_1(U_{10})f_2(r_0). \quad (1)$$

Ocean waves always exist on the sea surface. It is not reasonable to consider only the effects of sea surface winds while ignoring the effects of ocean waves. Zhao et al. (2006) provided a new wave state dependent SSGF and assumed that the shape of the droplet size spectrum is independent of wind speed and wind-wave state. Therefore, SSGF can be divided into two independent functions:

$$\frac{dF}{dr_0} = f_1(U_{10}, \omega_p)f_2(r_0), \quad (2)$$

where $f_1(U_{10}, \omega_p)$ is a function of wind and the circular frequency corresponding to the ocean wave spectrum peak (ω_p). Norris et

al. (2013a) also found the SSGF was influenced by wave breaking, and the SSGF was parameterized by the measured whitecap coverage.

2.2 SSGF based on whitecap coverage

2.2.1 Bubble-induced SSGF

The breaking bubbles can produce sea spray droplets, which are commonly called jet droplets and film droplets, and we call them bubble-induced droplets. Monahan et al. (1986) gave the SSGFs applicable to the bubble-induced droplets, based on the whitecap coverage, and the radius of droplets applicable to a relative humidity of 80% ranged from 0.8 μm to 10 μm .

$$\frac{dF}{dr_{80}} = \frac{W}{\tau_d} \frac{dE}{dr_{80}} = W \frac{1}{\tau_d} \frac{dE}{dr_{80}}, \quad (3)$$

where r_{80} is the droplet radius at a reference relative humidity of 80%, it should be pointed out that r_0 and r_{80} are different terms of spray droplets radius, and they can transform each other (Andreas, 1998; Veron, 2015). $\tau_d = 3.53$ s is the typical decay time of a whitecap, and W is the fractional coverage of whitecaps, which is a function of wind speed. $\frac{dE}{dr_{80}}$ is the number of droplets per increment of droplet radius generated during the decay of a unit area of whitecap, and Monahan et al. (1986) gave the expression of $\frac{dE}{dr_{80}}$:

$$\begin{aligned} \frac{dE}{dr_{80}} &= 1.262 \times 10^6 r_{80}^{-3} (1 + 0.057 r_{80}^{1.05}) \times 10^{1.19 \exp(-B^2)}, \\ B &= (0.380 - \lg r_{80}) / 0.650. \end{aligned} \quad (4)$$

Based on the SSGF constructed by Monahan et al. (1986), many researchers provided their revised bubble-induced SSGFs (Woolf et al., 1988; Gong, 2003).

It should be noted that the above SSGF are commonly referred to as discrete whitecap method (Callaghan, 2013), which determines the number of droplets produced per unit whitecap area, and assumes that the rate of production and the rate of decay of whitecap area per unit area sea surface were equal in conditions of steady state whitecap coverage. It is not the continuous whitecap method, which estimates the size-resolved number of droplets produced per unit whitecap area per second (Lewis and Schwartz, 2004).

2.2.2 Sea spume generation function

Droplets are produced not only by bubbles but also by the wind blowing across the wave tops. When the wind blows across the wave crests, droplets fall from the crest, and they are called spume droplets. These droplets have a larger radius than bubble-induced droplets. The sea spume generation function proposed by Fairall et al. (1994) can be expressed as:

$$\frac{dF}{dr_0} = Wf(r_0), \quad (5)$$

where $f(r_0)$ is the source spectrum per unit area of whitecap. This SSGF is used mainly to express the generation of spume droplets. Andreas (2002) gave the detailed relationship between the SSGF of Fairall et al. (1994) and Andreas (1992) in a review of the past SSGFs:

$$\frac{dF}{dr_0} = 38W(U_{10}) r_0^{-0.024} \left. \frac{dF_{A92}}{dr_{80}} \right|_{U_{10}=11}, \quad (6)$$

where $W(U_{10})$ is the whitecap coverage proposed by Monahan et al. (1986), which is only dependent on the 10 m wind speed. $\left. \frac{dF_{A92}}{dr_{80}} \right|_{U_{10}=11}$ is the SSGF proposed by Andreas (1992) when the sea surface wind speed at 10 m is equal to 11 m/s.

Equations (3)–(6) show that whitecap coverage is an important parameter used to construct an SSGF. However, the droplet size spectrum used by the bubble-induced droplets and spume droplets in SSGF is discontinuous, and the range of the initial radius of the droplets is usually divided into two parts (Shi et al., 2009). To establish the SSGF for a wider size range of droplets, researchers often use interpolation for the discontinuous parts of these two types of SSGFs (Shi et al., 2009; Liu et al., 2012). In fact, the size distribution of these two types of the droplets should be continuous in the process of droplet generation.

3 Model design

3.1 Parameterization of bubble-induced SSGF

The SSGF constructed by Monahan et al. (1986) using Eqs (3) and (4) has proven useful in many subsequent studies (Woolf et al., 1988; Gong, 2003). Woolf et al. (1988) updated the SSGF of Monahan et al. (1986), which is applicable to bubble-induced droplets, by using water tank observational data of whitecaps, and the updated $\frac{dE}{dr_{80}}$:

$$\frac{dE}{dr_{80}} = \exp \left[16.1 - 3.43 \lg r_{80} - 2.49 (\lg r_{80})^2 + 1.21 (\lg r_{80})^3 \right]. \quad (7)$$

The fitting relation in Eq. (7) is complicated, and the bubble-induced spray droplet size spectrum is different than the common expression for spume droplets. In this paper, the least square method is used for further fitting of Eq. (7) to obtain $\frac{dE}{dr_{80}}$ with a simpler expression:

$$\frac{dE}{dr_{80}} = 3.35 \times 10^6 r_{80}^{-3}, \quad R = 0.98, \quad (8)$$

where R is the correlation coefficient, and the size spectrum shape of bubble-induced sea spray droplets is simplified to r_0^{-3} . According to the relationship between r_{80} and r_0 in Andreas (2002):

$$r_{80} = 0.518 r_0^{0.976}. \quad (9)$$

Equation (8) is approximately:

$$\frac{dE}{dr_{80}} = 2.68 \times 10^7 r_0^{-3}. \quad (10)$$

Equation (10) is applicable to the droplets generated by bubbles, and the initial droplet radii are in the applicable range of $2 \mu\text{m} \leq r_0 \leq 20 \mu\text{m}$. Thus, the SSGF of droplets generated by bubbles can be expressed as:

$$\frac{dF}{dr_0} = A_1(W) r_0^{-3}, \quad 2 \mu\text{m} \leq r_0 \leq 20 \mu\text{m}, \quad (11)$$

where A_1 is a function of whitecap coverage (W , %):

$$A_1(W) = 3.80 \times 10^6 W. \quad (12)$$

3.2 Parameterization of the sea spume generation function

The sea spume generation function is often parameterized in the form of Eq. (1). Andreas (1998) gave the SSGF based on the data of Wu et al. (1984):

$$\frac{dF}{dr_{80}} = \begin{cases} C_1(U_{10}) r_{80}^{-1}, & 10 \mu\text{m} \leq r_{80} < 37.5 \mu\text{m}, \\ C_2(U_{10}) r_{80}^{-2.8}, & 37.5 \mu\text{m} \leq r_{80} < 100 \mu\text{m}, \\ C_3(U_{10}) r_{80}^{-8}, & 100 \mu\text{m} \leq r_{80} \leq 250 \mu\text{m}, \end{cases} \quad (13)$$

where C_1 , C_2 and C_3 are functions of wind speed at a height of 10 m on the sea surface. Andreas (1998) determined the value of C_1 , C_2 and C_3 based on the calculated value of SSGF at $U_{10} = 15$ m/s which proposed by Smith et al. (1993), and $C_1 = 1.955 \times 10^3$, $C_2 = 1.331 \times 10^6$, and $C_3 = 3.344 \times 10^{16}$.

Considering the relationship between whitecap coverage, W , and wind speed, Eq. (13) can be expressed as:

$$\frac{dF}{dr_0} = \begin{cases} A_2(W) r_0^{-1}, & 20 \mu\text{m} \leq r_0 < 75 \mu\text{m}, \\ A_3(W) r_0^{-2.8}, & 75 \mu\text{m} \leq r_0 < 200 \mu\text{m}, \\ A_4(W) r_0^{-8}, & 200 \mu\text{m} \leq r_0 \leq 500 \mu\text{m}, \end{cases} \quad (14)$$

where A_2 , A_3 and A_4 are functions of whitecap coverage. Equation (14) is the sea spume generation function dependent on whitecap coverage, and the initial droplet radii are in the applicable range of $20 \mu\text{m} \leq r_0 \leq 500 \mu\text{m}$.

3.3 New sea spray generation function

Combining the bubble-induced SSGF and the sea spume generation function, a wider size range SSGF can be constructed that includes the radii of the two kinds of droplets. Based on Eqs (11) and (14), the new SSGF related to the whitecap coverage is obtained:

$$\frac{dF}{dr_0} = \begin{cases} A_1(W) r_0^{-3}, & 2 \mu\text{m} \leq r_0 < 20 \mu\text{m}, \\ A_2(W) r_0^{-1}, & 20 \mu\text{m} \leq r_0 < 75 \mu\text{m}, \\ A_3(W) r_0^{-2.8}, & 75 \mu\text{m} \leq r_0 < 200 \mu\text{m}, \\ A_4(W) r_0^{-8}, & 200 \mu\text{m} \leq r_0 < 500 \mu\text{m}. \end{cases} \quad (15)$$

When Andreas (1998) produced the SSGF with Eq. (13), he believed that the SSGF was continuous. Therefore, C_1 was determined first, and then C_2 and C_3 were determined. Using the same method, based on Eq. (11), A_1 can be determined first, then A_2 , A_3 and A_4 can be obtained. Thus, Eq. (15) can be converted into Eq. (16):

$$\frac{dF}{dr_0} = \begin{cases} 3.80 \times 10^6 W r_0^{-3}, & 2 \mu\text{m} \leq r_0 < 20 \mu\text{m}, \\ 9.50 \times 10^3 W r_0^{-1}, & 20 \mu\text{m} \leq r_0 < 75 \mu\text{m}, \\ 2.25 \times 10^7 W r_0^{-2.8}, & 75 \mu\text{m} \leq r_0 < 200 \mu\text{m}, \\ 2.08 \times 10^{19} W r_0^{-8}, & 200 \mu\text{m} \leq r_0 < 500 \mu\text{m}. \end{cases} \quad (16)$$

Equation (16) is the new SSGF covering the initial droplet radii of 2–500 μm , which is related to the whitecap coverage. It can describe the generation of bubble-induced droplets and spume droplets. It is shown that the spectrum shape of the

droplet size spectrum is divided into four continuous sections. The whitecap coverage W is usually parameterized by wind speed or wave state parameters (Zhao and Toba, 2001; Ren et al., 2016).

4 Results

4.1 The effect of wind speed is considered

Monahan and Muircheartaigh (1980) gave the relationship between whitecap coverage and 10 m wind speed:

$$W = 3.8 \times 10^{-6} U_{10}^{3.4}. \quad (17)$$

However, the relationship between whitecap coverage and wind speed varies according to different data analysis results (Ren et al., 2016). Zhao and Toba (2001) obtained the whitecap coverage related only to wind speed by analyzing laboratory and field data:

$$W = 2.98 \times 10^{-5} U_{10}^{4.04}. \quad (18)$$

These two whitecap coverage Eqs (17) and (18) that depend only on the wind speed are substituted into the new SSGF, which is expressed by Eq. (16). The wind speed, U_{10} , is taken as 15 m/s, and the change results of the SSGFs with the initial radius of the droplet are obtained, as shown in Fig. 1.

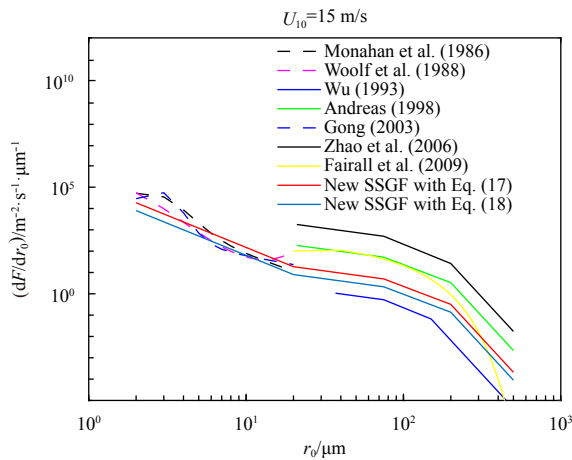


Fig. 1. Comparison of SSGFs by Eqs (17) and (18) with those of Monahan et al. (1986), Woolf et al. (1988), Wu (1993), Andreas (1998), Gong (2003), Zhao et al. (2006) with $R_B = 2.84 \times 10^4$, and Fairall et al. (2009) with 10 m fetch, at $U_{10} = 15$ m/s.

In Fig. 1, the results of new SSGF using Eq. (18) are smaller than those obtained with Eq. (17). Within the size range of bubble-induced droplets, it is found that the SSGFs of Monahan et al. (1986), Woolf et al. (1988) and Gong (2003) are close to each other, and the new SSGF using Eq. (17) is the average state of these studies. In the main spume-droplet stage, the SSGFs of Andreas (1998) and Fairall et al. (2009) are close to each other as well, and the new SSGFs with Eqs (17) and (18) are in the middle of the calculation results of the SSGFs of Andreas (1998), Fairall et al. (2009), and Wu (1993). Due to the discrete relationship between whitecap coverage and wind speed, the calculated value of the SSGF has a wide range of changes, which is generally believed by researchers to be caused by not considering the effects

of waves (Zhao and Toba, 2001; Lafan et al., 2007).

4.2 The effect of waves is considered

The SSGF is not only related to the wind but also to the wave state. The whitecap coverage in Eqs (17) and (18) is related only to the wind speed. Zhao and Toba (2001) also pointed out that the wave state parameter, R_B , could fit the whitecap coverage reasonably, and gave the relationship of W and R_B .

$$W = 3.88 \times 10^{-5} R_B^{1.09}, \quad (19)$$

where $R_B = u_*^2 / \omega_p \nu_a$ is called the windsea Reynolds number, which is proposed by Toba and Koga (1986) firstly. The wave spectrum peak frequency is $\omega_p = 2\pi/T_s$, and T_s is the significant wave period, and ν_a is the kinematic viscosity of air. Windsea Reynolds number R_B is regarded as a parameter describing the intensity of air-sea interaction, and contains both wind (u_*) and peak frequency (ω_p) information. Windsea Reynolds number R_B can also be written as $R_B = C_D \frac{U_{10}^3}{g \nu_a} \beta$ and $\beta = \frac{g}{\omega_p U_{10}}$ is called the wave age. In order to facilitate the calculation, we adopt the drag coefficient $C_D = (0.8 + 0.065 U_{10}) \times 10^{-3}$, and u_* is the friction velocity, which can be written as $u_* = U_{10} C_D^{1/2}$ (Wu, 1982).

By comparing Eqs (17), (18) and (19), as shown in Fig. 2, it can be found that under different wave states, the calculation results of Eq. (19) cover the calculation results of Eq. (17). At the same time, when U_{10} is greater than 6 m/s, the calculation results of Eq. (19) cover the calculation results of Eq. (18). Thus, the influence of wave state on whitecap coverage cannot be ignored, and R_B is better than wind speed to parameterize the coupling effects of wind and waves at the air-sea interface. Since windsea Reynolds number R_B is a wind-wave parameter (Toba and Koga, 1986; Zhao and Toba, 2001), it is not applicable to the swell-dominated seas, and it cannot be used when wave age is much larger than 1.

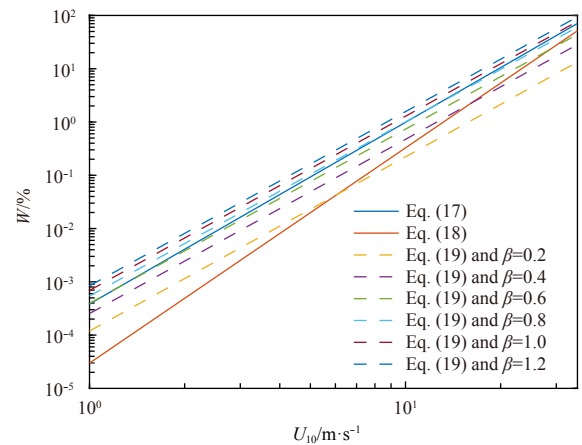


Fig. 2. Whitecap coverage versus 10 m wind speed (U_{10}) at different wave ages.

Based on Eqs (16) and (19), the relationship between the new SSGF and the wave state is established. Therefore, the results of the new SSGF for different wave ages can be analyzed. Figure 3 shows the comparison between the SSGF and R_B for different wave ages. It can be seen that the new SSGF with Eq. (19) increases with increasing wind speed, and it increases more rapidly than the new SSGFs with Eqs (17) and (18). Meanwhile, the

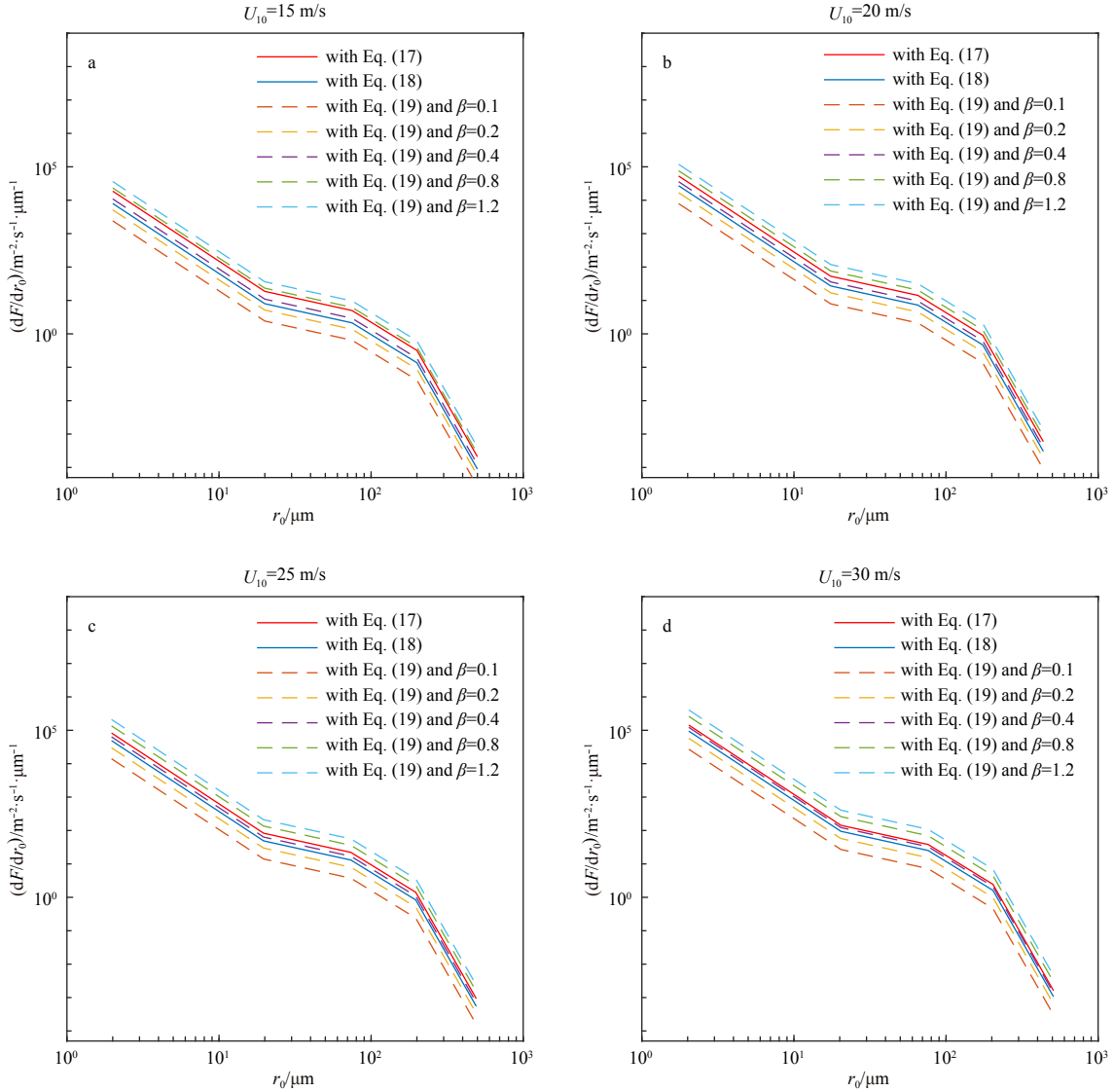


Fig. 3. Comparison of the calculated results of the new SSGF with Eqs (17), (18) and (19) under different wave ages at four wind speeds. a. The wind speed $U_{10}=15$ m/s, b. the wind speed $U_{10}=20$ m/s, c. the wind speed $U_{10}=25$ m/s, and d. the wind speed $U_{10}=30$ m/s.

result of the new SSGF with Eq. (19) can cover the value of the new SSGFs with Eqs (17) and (18), which means that the new SSGF with Eq. (19) can express the effect of ocean waves.

Fairall et al. (2009) measured the amount of sea spray droplets in a water tank at different wind speeds. His paper (Fig. 5a in the literature of Fairall et al. (2009)) shows the distribution of the number of droplets with the initial radius of droplets under weak wind conditions (Fairall et al., 2009; Wan et al., 2017). These data can be obtained from the website (ftp.etl.noaa.gov/BLO/air-sea/onr_droplet/CIP_tunnel_03/processed), in which 49 groups of data were processed. In this paper, four groups of data similar to those measured under the weak wind conditions of Fig. 5a in the literature of Fairall et al. (2009) are selected for comparison (As mentioned by Fairall et al. (2009), the weak wind data was used to analyze the sea spray generation on 6 February. We analyze the data come from above website, and find that there are only four groups of data were measured in the water tank on 6 February with a weak wind force of 13.9 m/s). The wind speed U_{10} is calculated by an iterative method. To reduce the error,

when the amount of droplets within a certain initial radius is fewer than 3, that data bin is not used, as shown in Table 1.

The SSGF corresponding to the measurement data is calculated using the relationship between SSGF and the number concentration of droplets given by Andreas (2004):

$$\frac{dF}{dr_0} = u_f(r_0) \frac{dN}{dr_0}, \quad (20)$$

where $u_f(r_0)$ is terminal falling speed of droplets, and $\frac{dN}{dr_0}$ is number concentration of these droplets, which was measured by Fairall et al. (2009). Therefore, to obtain the $\frac{dF}{dr_0}$ values corresponding to the measurement data, we need to know $u_f(r_0)$.

Norris et al. (2013a) gave the SSGF based on the field observational data:

$$\frac{dF}{dr_{80}} = W \times \left(\frac{dF_p}{dr_{80}} \right), \quad (21)$$

Table 1. The reanalyzed four groups of data on 6 February

Experiment number	Amount of data bin	$u_*/\text{m}\cdot\text{s}^{-1}$	$U_{10}/\text{m}\cdot\text{s}^{-1}$	Observation height/m
01	27	1.59	31	0.150
02	34	1.76	33	0.125
03	27	1.40	28	0.195
04	16	1.22	25	0.275

where F_p is the flux of droplets generated by per unit whitecap area, which can be calculated from the number concentration of droplets and the friction velocity:

$$\frac{dF_p}{dr_{80}} = \left(\frac{dN}{dr_{80}} \right) u_*. \quad (22)$$

By combining Eqs (21), (22) and (9), $\frac{dF}{dr_0}$ is expressed as:

$$\frac{dF}{dr_0} = Wu_* \times \left(\frac{dN}{dr_0} \right). \quad (23)$$

Therefore, the approximate expression of the terminal falling speed of droplets can be obtained from Eqs (20) and (23):

$$u_f(r_0) = Wu_*. \quad (24)$$

Zhao and Toba (2001) gave the relationship between whitecap coverage and friction velocity with laboratory and field data:

$$W = 8.59u_*^{3.42}. \quad (25)$$

Therefore, we can give the expression of the terminal falling speed of droplets with friction velocity:

$$u_f(r_0) = 0.0859u_*^{4.42}. \quad (26)$$

The measured data are reanalyzed by Eq. (20), and $\frac{dF}{dr_0}$ is obtained.

The reanalysis measurement results were compared with the

new SSGF with Eqs (17) and (18) in Fig. 4. It shows that they do not correspond very well to the discrete SSGF values. Discrete SSGF values represent the effects of different wave states (Zhao and Toba, 2001; Zhao et al., 2006). Since whitecap coverage is parameterized by R_B , the calculation results of new SSGF with Eq. (19) under different wave ages can be analyzed. As shown in Fig. 4, the new SSGF with Eq. (19) covers the measured values at different wave ages. However, when $U_{10} > 30$ m/s, the results of the new SSGF are not close to the observational data for the larger droplets. This is because Eqs (17), (18) and (19) are fitted with the data at U_{10} which is less than 30 m/s. Therefore, there is a certain error in the application of U_{10} with wind speeds greater than 30 m/s. Meanwhile, it can be seen that, at $U_{10} = 25$ m/s, the new SSGF with Eq. (19) is not close to the larger droplets.

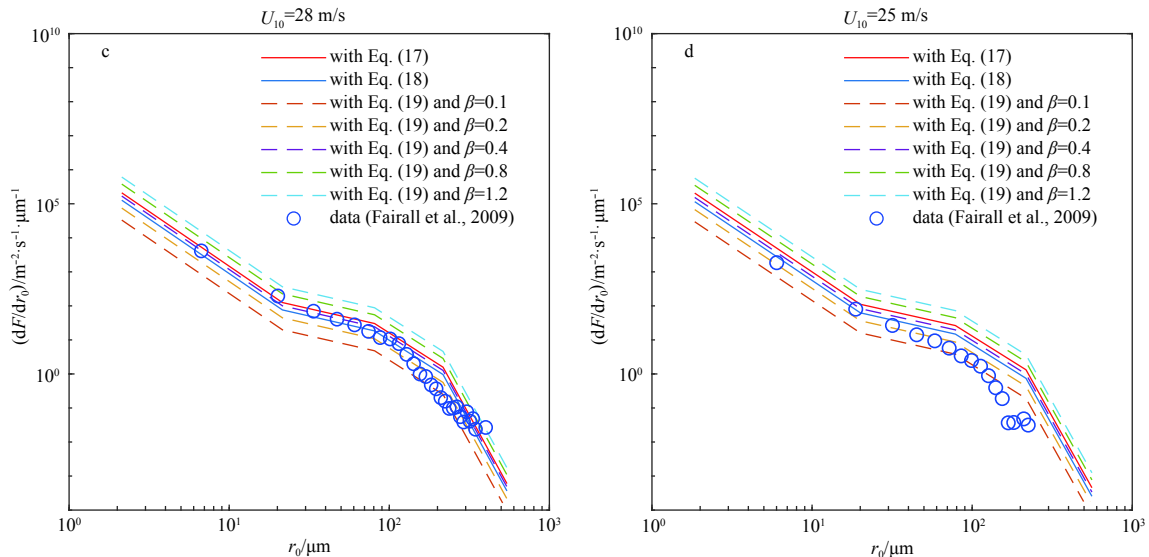
5 Discussion

Zhao and Toba (2001) also gave the parameterization formula of W based on another wave state parameter, R_H :

$$W = 4.02 \times 10^{-5} R_H^{0.96}, \quad (27)$$

where $R_H = u_* H_s / \nu$ and H_s is the significant wave height. Norris et al. (2013b) give a similar wave parameter, $R_{HW} = u_* H_s / \nu_w$, where ν_w is the kinematic viscosity of water. R_B can be used to parameterize the SSGF and R_H is also used to parameterize the SSGF (Zhao and Toba, 2001).

Since both wave state parameters R_B and R_H are established under wind-wave conditions (Toba and Koga, 1986; Zhao and Toba, 2001; Troitskaya et al., 2018), the relationship between them can be established by the theory of the wind-wave local equilibrium law (Toba et al., 1990):

**Fig. 4.**

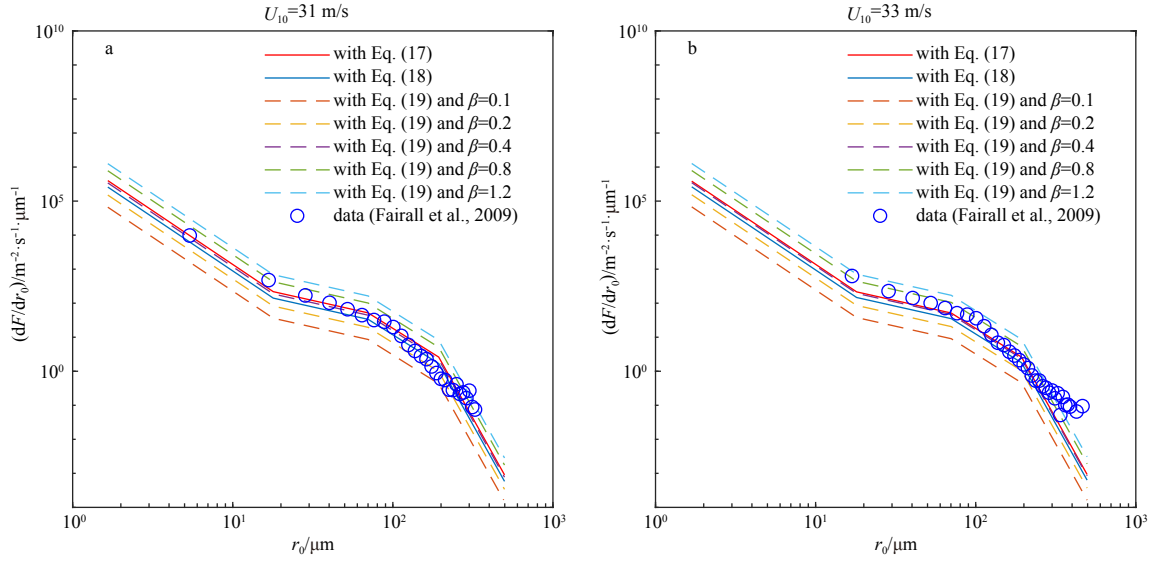


Fig. 4. Comparison of the observational data and calculated results of the new SSGF with Eqs (17), (18) and (19) under different wave ages with four groups of observational data. a. The first group of observational data, at $U_{10}=31$ m/s; b. the second group of observational data, at $U_{10}=33$ m/s; c. the third group of observational data, at $U_{10}=28$ m/s; and d. the fourth group of observational data, at $U_{10}=25$ m/s.

$$gH_s/u_*^2 = B(gT_s/u_*)^{3/2}, \quad (28)$$

where $B (= 0.062)$ is a constant. Based on Eq. (28), the corresponding relationship between R_B and R_H can be expressed as:

$$R_H = B \left(\frac{2\pi}{1.05} \right)^{3/2} C_d^{-1/4} \beta^{1/2} R_B. \quad (29)$$

Figure 5 shows that the calculation results of new SSGF for different wave ages, and it can be seen that new SSGF using Eq. (27) covers the measured values for different wave ages. Comparing Fig. 5 with Fig. 2, the results of the new SSGF using Eq. (27) are smaller than for the new SSGF with Eq. (19) at small wave ages. When $U_{10} > 30$ m/s, the results of the new SSGF are not

close to the observed data for the larger droplets as well. However, at $U_{10}=25$ m/s, the new SSGF using Eq. (27) results are better than those using Eq. (19).

R_B and R_H are the wave state parameters, but there are different values in different wave ages, as shown in Fig. 6. With the increasing wind speed, R_H is more discrete than R_B in different wave ages, which means that the R_H is more sensitive to wave effect than R_B , so the parameterization of whitecap coverage with R_H will have a better effect. Another wave state parameter, R_{Hw} , is mainly different from R_H in the kinematic viscosity coefficient (Norris et al., 2013b), but the dispersion degree of R_{Hw} and U_{10} is similar to that of R_H and U_{10} .

Figures 4–6 show that the new SSGF using wind-dependent whitecap coverage cannot express the spray-droplet generation under different wave states. The new SSGF with whitecap cover-

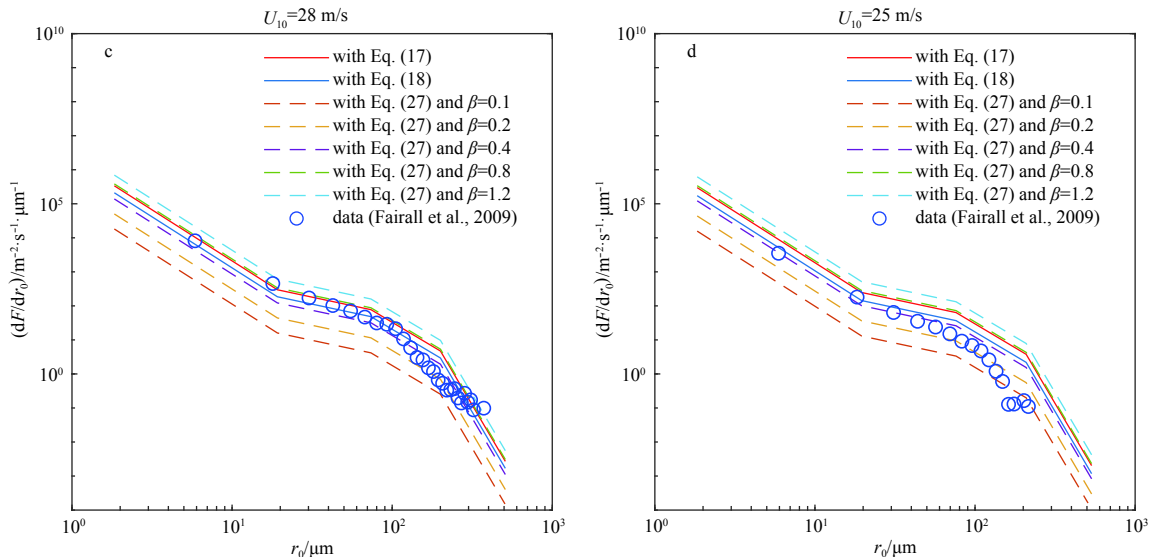


Fig. 5.

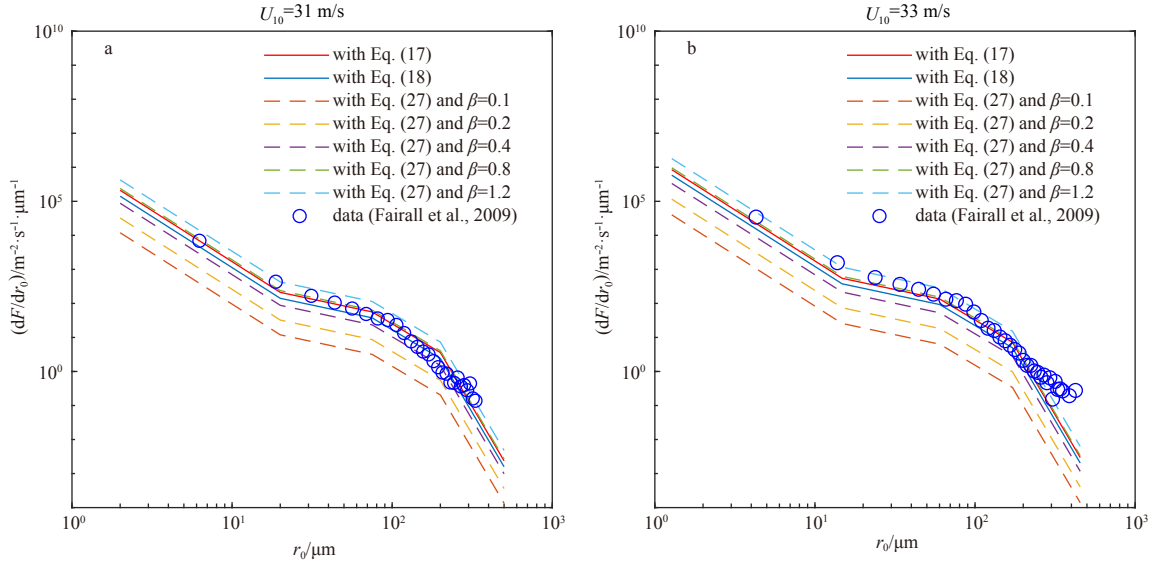


Fig. 5. Comparison of the observational data and calculated results of the new SSGF with Eqs (17), (18) and (27) under different wave ages with four groups observational data. a. The first group of observational data, at $U_{10}=31$ m/s; b. the second group of observational data, at $U_{10}=33$ m/s; c. the third group of observational data, at $U_{10}=28$ m/s; and d. the fourth group of observational data, at $U_{10}=25$ m/s.

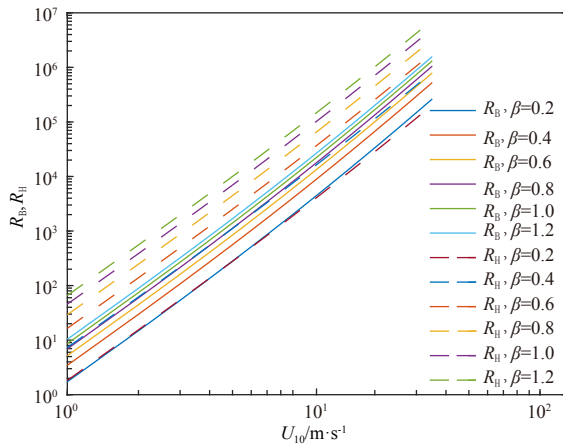


Fig. 6. R_B and R_H versus U_{10} with different wave age.

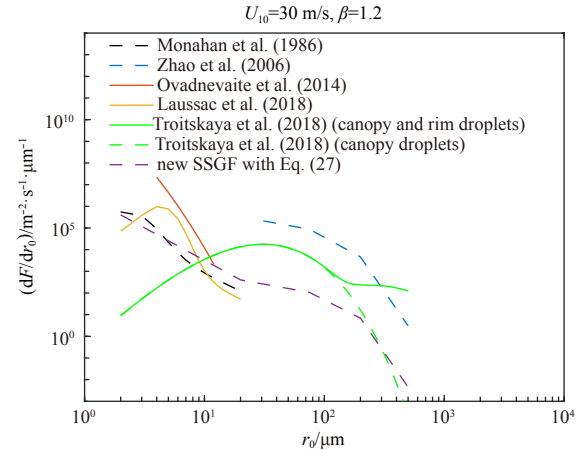


Fig. 7. Comparison of SSGFs considering wave effect.

age considering the wave state can better express the spray-droplet generation under different wind speeds and wave state conditions, and the calculated results of the SSGF are slightly different for different wave ages with different wave state parameters. In general, an SSGF dependent on wave state better describes the generation of spray droplets than an SSGF dependent on wind speed.

In order to analyze SSGF considering wave effect, the SSGF proposed by Zhao et al. (2006), Ovadnevaite et al. (2014), Laussac et al. (2018) and Troitskaya et al. (2018) are compared. In comparison, the wind speed is 30 m/s, and the wave age is 1.2, which means that the waves are fully developed, and the spray droplets are abundant. As shown in Fig. 7, when the spray droplets radius is small, the SSGF of Ovadnevaite et al. (2014), Laussac et al. (2018) and new SSGF with Eq. (27) are relatively close, while SSGF proposed by Ovadnevaite et al. (2014) is relatively high. The SSGF of Troitskaya et al. (2018), derived from theoretical model, cannot well simulate the generation of droplets

when the radius of droplets is less than 10 μm . When the radius of droplets is more than 100 μm , the trend of SSGF proposed by Troitskaya et al. (2018) is obviously different from common parameterized schemes. This is because the SSGF of Troitskaya et al. (2018) consists of two parts, namely canopy droplets with small droplet radius and rim droplets with large droplet radius. When droplets are larger than 100 μm , rim droplets dominate, and at this time, the SSGF of Troitskaya et al. (2018) do not follow size spectrum proposed by Monahan et al. (1986). The SSGF of Zhao et al. (2006) focuses on spume droplets, but by using this scheme, there will be discontinuous with the current bubble-induced SSGF (Shi et al., 2009, 2016; Liu et al., 2012).

The aerosol and air-sea flux can be calculated with SSGF. When the global aerosol and air-sea flux modelling is carried out using the new SSGF with whitecap coverage considering the wave state in this paper, the flux depends not only on wind speed but also on wave state, and the flux will be different under different wave state, especially in the sea dominated by wind-waves.

For example, under the same wind speed conditions, when the wave age is large, that is, the more mature wind-waves will produce more droplets. Therefore, based on the new SSGF dependent on wave state, the global aerosol and air-sea flux can be modeled in combination with wave numerical model. The main purpose of this paper is to parameterize a new SSGF which is dependent on wave state, and the related aerosol and air-sea flux modelling work will be carried out in the future.

6 Conclusions

Whitecap coverage is an important manifestation of the wave breaking process, and is related to wind speed. Meanwhile, some researchers believe that whitecap coverage is related to wave state. In this paper, an SSGF using a wider range of droplet sizes and dependent on whitecap coverage is parameterized, and the whitecap coverage related to wind speeds and wave states is used to calculate the new SSGF.

Combining the bubbled-induced SSGF and sea spume generation function, a wider size range SSGF can be constructed including the radii of the bubble-induced droplets and the spume droplets. Equation (16) is the new SSGF covering the initial droplet radii in a range of 2–500 μm , which is related to the whitecap coverage, and it can describe the generation of two kinds of droplets.

The comparison between the calculated results and the measured results shows that the calculated results of the new SSGF with Eqs (17) and (18) related only to wind speed cannot effectively describe the generation of spray droplets. The new SSGF with Eqs (19) and (27) considering the wave effects can better describe the droplet generation process under different wave states. Thus, the new SSGF is sensitive to wave effects.

Both R_B and R_H are related to wave state, but the calculated results are different, which indicates that a reasonable selection of wave state parameters and the parameterization of whitecap coverage have an impact on the new SSGF. It is necessary to further analyze the relationships between whitecap coverage and the wave state parameters to find more reasonable wave state parameters for parameterization of whitecap coverage. In this paper, based on comparisons with observational data in the laboratory, the new SSGF (Eq. (16)) with Eq. (27) is recommended.

Acknowledgements

We thank C.W. Fairall for his observational data in the laboratory.

References

- Andreas E L. 1992. Sea spray and the turbulent air-sea heat fluxes. *Journal of Geophysical Research: Oceans*, 97(C7): 11429–11441, doi: [10.1029/92JC00876](https://doi.org/10.1029/92JC00876)
- Andreas E L. 1998. A new sea spray generation function for wind speeds up to 32 $\text{m}\cdot\text{s}^{-1}$. *Journal of Physical Oceanography*, 28(11): 2175–2184, doi: [10.1175/1520-0485\(1998\)028<2175:ANSSGF>2.0.CO;2](https://doi.org/10.1175/1520-0485(1998)028<2175:ANSSGF>2.0.CO;2)
- Andreas E L. 2002. A review of the sea spray generation function for the open ocean. In: Perrie W, ed. *Atmosphere–Ocean Interactions*. Southampton: WIT Press, 1–46
- Andreas E L. 2004. Spray stress revisited. *Journal of Physical Oceanography*, 34(6): 1429–1440, doi: [10.1175/1520-0485\(2004\)034<1429:SSR>2.0.CO;2](https://doi.org/10.1175/1520-0485(2004)034<1429:SSR>2.0.CO;2)
- Andreas E L, Edson J B, Monahan E C, et al. 1995. The spray contribution to net evaporation from the sea: a review of recent progress. *Boundary-Layer Meteorology*, 72(1–2): 3–52
- Barthel S, Tegen I, Wolke R. 2019. Do new sea spray aerosol source functions improve the results of a regional aerosol model?. *Atmospheric Environment*, 198: 265–278, doi: [10.1016/j.atmosenv.2018.10.016](https://doi.org/10.1016/j.atmosenv.2018.10.016)
- Callaghan A H. 2013. An improved whitecap timescale for sea spray aerosol production flux modeling using the discrete whitecap method. *Journal of Geophysical Research: Atmospheres*, 118(17): 9997–10010, doi: [10.1002/jgrd.50768](https://doi.org/10.1002/jgrd.50768)
- Fairall C W, Banner M L, Peirson W L, et al. 2009. Investigation of the physical scaling of sea spray spume droplet production. *Journal of Geophysical Research: Oceans*, 114(C10): C10001, doi: [10.1029/2008JC004918](https://doi.org/10.1029/2008JC004918)
- Fairall C W, Kepert J D, Holland G J. 1994. The effect of sea spray on surface energy transports over the ocean. *The Global Atmosphere and Ocean System*, 2: 121–142
- Gong S L. 2003. A parameterization of sea-salt aerosol source function for sub- and super-micron particles. *Global Biogeochemical Cycles*, 17(4): 1097
- Lafon C, Piazzola J, Forget P, et al. 2007. Whitecap coverage in coastal environment for steady and unsteady wave field conditions. *Journal of Marine Systems*, 66(1–4): 38–46
- Laussac S, Piazzola J, Tedeschi G, et al. 2018. Development of a fetch dependent sea-spray source function using aerosol concentration measurements in the North-Western Mediterranean. *Atmospheric Environment*, 193: 177–189, doi: [10.1016/j.atmosenv.2018.09.009](https://doi.org/10.1016/j.atmosenv.2018.09.009)
- Lewis E R, Schwartz S E. 2004. *Sea Salt Aerosol Production: Mechanisms, Methods, Measurements and Models-A Critical Review*. Washington: American Geophysical Union
- Ling S C, Saad A I, Kao T W. 1980. Microdroplets and transport of moisture from ocean. *Journal of the Engineering Mechanics Division*, 106(6): 1327–1339
- Liu Bin, Guan Changlong, Xie Lian. 2012. The wave state and sea spray related parameterization of wind stress applicable from low to extreme winds. *Journal of Geophysical Research: Oceans*, 117(C11): C00J22
- Liu Bin, Liu Huiqing, Xie Lian, et al. 2011. A coupled atmosphere–wave–ocean modeling system: Simulation of the intensity of an idealized tropical cyclone. *Monthly Weather Review*, 139(1): 132–152, doi: [10.1175/2010MWR3396.1](https://doi.org/10.1175/2010MWR3396.1)
- Monahan E C, Muircheartaigh I Ó. 1980. Optimal power-law description of oceanic whitecap coverage dependence on wind speed. *Journal of Physical Oceanography*, 10(12): 2094–2099, doi: [10.1175/1520-0485\(1980\)010<2094:OPLDOO>2.0.CO;2](https://doi.org/10.1175/1520-0485(1980)010<2094:OPLDOO>2.0.CO;2)
- Monahan E C, Spiel D E, Davidson K L. 1986. A model of marine aerosol generation via whitecaps and wave disruption. In: Monahan E C, Niocaill G M, eds. *Oceanic Whitecaps*. Dordrecht: Springer, 167–174.
- Mueller J A, Veron F. 2009. A sea state-dependent spume generation function. *Journal of Physical Oceanography*, 39(9): 2363–2372, doi: [10.1175/2009JPO4113.1](https://doi.org/10.1175/2009JPO4113.1)
- Norris S J, Brooks I M, Moat B I, et al. 2013a. Near-surface measurements of sea spray aerosol production over whitecaps in the open ocean. *Ocean Science*, 9(1): 133–145
- Norris S J, Brooks I M, Salisbury D J. 2013b. A wave roughness Reynolds number parameterization of the sea spray source flux. *Geophysical Research Letters*, 40(16): 4415–4419
- Ovadnevaite J, Manders A, De Leeuw G, et al. 2014. A sea spray aerosol flux parameterization encapsulating wave state. *Atmospheric Chemistry and Physics*, 14(4): 1837–1852, doi: [10.5194/acp-14-1837-2014](https://doi.org/10.5194/acp-14-1837-2014)
- Ren Danqin, Hua Feng, Yang Yongzeng, et al. 2016. The improved model of estimating global whitecap coverage based on satellite data. *Acta Oceanologica Sinica*, 35(5): 66–72, doi: [10.1007/s13131-016-0848-3](https://doi.org/10.1007/s13131-016-0848-3)
- Rizza U, Canepa E, Ricchi A, et al. 2018. Influence of wave state and sea spray on the roughness length: feedback on medicanes. *Atmosphere*, 9(8): 301, doi: [10.3390/atmos9080301](https://doi.org/10.3390/atmos9080301)
- Shao Weizeng, Sheng Yexin, Li Huan, et al. 2018. Analysis of wave distribution simulated by WAVEWATCH-III model in typhoons passing Beibu Gulf, China. *Atmosphere*, 9(7): 265, doi: [10.3390/atmos9070265](https://doi.org/10.3390/atmos9070265)
- Sheng Yexin, Shao Weizeng, Li Shuiqing, et al. 2019. Evaluation of

- typhoon waves simulated by WaveWatch-III model in shallow waters around Zhoushan islands. *Journal of Ocean University of China*, 18(2): 365–375, doi: [10.1007/s11802-019-3829-2](https://doi.org/10.1007/s11802-019-3829-2)
- Shi Jian, Zhao Dongliang, Li Xunqiang, et al. 2009. New wave-dependent formulae for sea spray flux at air-sea interface. *Journal of Hydrodynamics*, 21(4): 573–581, doi: [10.1016/S1001-6058\(08\)60186-9](https://doi.org/10.1016/S1001-6058(08)60186-9)
- Shi Jian, Zhong Zhong, Li Ruijie, et al. 2011. Dependence of sea surface drag Coefficient on wind-wave Parameters. *Acta Oceanologica Sinica*, 30(2): 14–24, doi: [10.1007/s13131-011-0101-z](https://doi.org/10.1007/s13131-011-0101-z)
- Shi Jian, Zhong Zhong, Li Xunqiang, et al. 2016. The influence of wave state and sea spray on drag coefficient from low to high wind speeds. *Journal of Ocean University of China*, 15(1): 41–49, doi: [10.1007/s11802-016-2655-z](https://doi.org/10.1007/s11802-016-2655-z)
- Smith M H, Park P M, Consterdine I E. 1993. Marine aerosol concentrations and estimated fluxes over the sea. *Quarterly Journal of the Royal Meteorological Society*, 119(512): 809–824, doi: [10.1002/qj.49711951211](https://doi.org/10.1002/qj.49711951211)
- Toba Y, Iida N, Kawamura H, et al. 1990. Wave dependence of sea-surface wind stress. *Journal of Physical Oceanography*, 20(5): 705–721, doi: [10.1175/1520-0485\(1990\)020<0705:WDOSSW>2.0.CO;2](https://doi.org/10.1175/1520-0485(1990)020<0705:WDOSSW>2.0.CO;2)
- Toba Y, Koga M. 1986. A parameter describing overall conditions of wave breaking, whitecapping, sea-spray production and wind stress. In: Monahan E C, Niocaill G M, eds. *Oceanic Whitecaps*. Dordrecht: Springer, 37–47
- Troitskaya Y, Kandaurov A, Ermakova O, et al. 2018. The “bag break-up” spume droplet generation mechanism at high winds. Part I: Spray generation function. *Journal of Physical Oceanography*, 48(9): 2167–2188, doi: [10.1175/JPO-D-17-0104.1](https://doi.org/10.1175/JPO-D-17-0104.1)
- Veron F. 2015. Ocean spray. *Annual Review of Fluid Mechanics*, 47: 507–538, doi: [10.1146/annurev-fluid-010814-014651](https://doi.org/10.1146/annurev-fluid-010814-014651)
- Veron F, Hopkins C, Harrison E L, et al. 2012. Sea spray spume droplet production in high wind speeds. *Geophysical Research Letters*, 39(16): L16602
- Wan Zhanhong, Zhu Jianbin, Sun Ke, et al. 2017. An integrated turbulent simulation and parameter modeling study on sea-spray dynamics and fluxes. *Ocean Engineering*, 130: 64–71, doi: [10.1016/j.oceaneng.2016.11.041](https://doi.org/10.1016/j.oceaneng.2016.11.041)
- Woolf D K, Monahan E C, Spiel D E. 1988. Quantification of the marine aerosol produced by whitecaps. In: *Proceedings of the Seventh Conference on Ocean-Atmosphere Interaction*. Anaheim: American Meteorological Society, 182–185
- Wu Jin. 1982. Wind-stress coefficients over sea surface from breeze to hurricane. *Journal of Geophysical Research: Oceans*, 87(C12): 9704–9706, doi: [10.1029/JC087iC12p09704](https://doi.org/10.1029/JC087iC12p09704)
- Wu Jin. 1993. Production of spume drops by the wind tearing of wave crests: the search for quantification. *Journal of Geophysical Research: Oceans*, 98(C10): 18221–18227, doi: [10.1029/93JC01834](https://doi.org/10.1029/93JC01834)
- Wu Jin, Murray J J, Lai R J. 1984. Production and distributions of sea spray. *Journal of Geophysical Research: Oceans*, 89(C5): 8163–8169, doi: [10.1029/JC089iC05p08163](https://doi.org/10.1029/JC089iC05p08163)
- Wu Lichuan, Rutgersson A, Sahlée E, et al. 2015. The impact of waves and sea spray on modelling storm track and development. *Tellus A*, 67(1): 27967, doi: [10.3402/tellusa.v67.27967](https://doi.org/10.3402/tellusa.v67.27967)
- Zhao Dongliang, Toba Y. 2001. Dependence of whitecap coverage on wind and wind-wave properties. *Journal of Oceanography*, 57(5): 603–616, doi: [10.1023/A:1021215904955](https://doi.org/10.1023/A:1021215904955)
- Zhao Dongliang, Toba Y, Sugioka K I, et al. 2006. New sea spray generation function for spume droplets. *Journal of Geophysical Research: Oceans*, 111(C2): C02007